

Slope Failure due to Ground Water Level Change in Centrifuge

National Institute of Occupational Safety and Health ○ Timpong Sahaphol, Itoh Kazuya and Toyosawa Yasuo

1. Introduction

In Japan, the rainfall-induced slope failure is one of the most destructive natural disasters, causing significant property damage and loss of life. In general natural slopes are in unsaturated condition and the ground water level is relatively deep, an increase of ground water level due to rainwater infiltration into the slope during heavy rainfall periods can cause the generation of positive pore water pressure, increases soil weight and decreases shear strength of soil, which can significantly making the slope more susceptible to failure.

2. Centrifuge modelling

In this paper, the model slope test was performed in the NIIS Mark-II centrifuge to investigate the mechanism of slope failure induced by ground water change. A rigid aluminum model test container with acrylic transparent wall on one side was constructed to allow the visual observation of model slope during the centrifuge test. The internal dimensions of the container are 25 cm wide, 80 cm long and 70 cm high. The container was divided into three sections; a central portion for making the model slope, a water supply chamber and a drain chamber. These sections were separated by perforated steel walls covered with wire mesh to allow the water

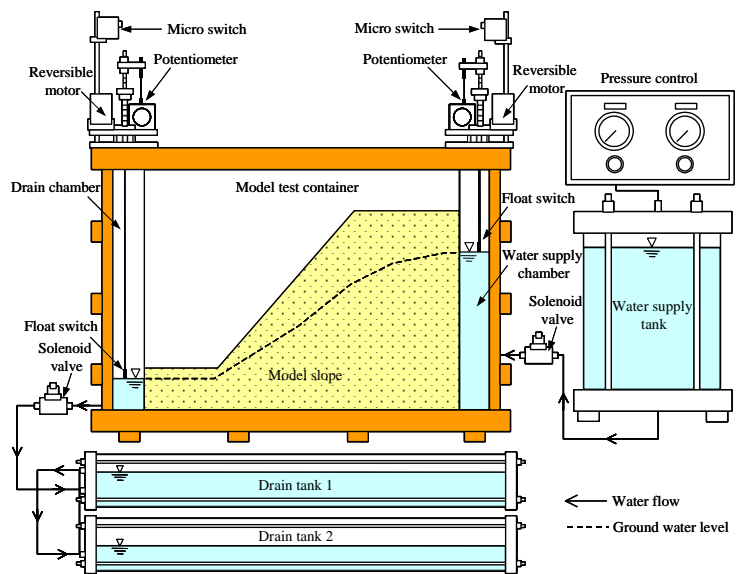


Fig. 1. The in-flight ground water control system

flow in and flow out of the model slope without migration of soil particle. Figure 1 shows the in-flight ground water control system, which is capable of simulating the infiltration from rainfall to bring the ground water to the particular level during the centrifuge test. The control system consists of water supply and drain tanks, pressure control system, reversible motors, float switches, two-port solenoid valves, limit micro switches and potentiometer-type displacement transducers. The water level in the water supply and the drain chambers can be controlled in real-time by the computer. The model slope was prepared by mixing River sand with Fujinomori clay as a ratio of 9:1 by weight at water content of 15%. The physical properties of soil mixture are specific gravity $G_s = 2.65$, mean particle size $D_{50} = 0.25$ mm, minimum dry density $\rho_{d(\min)} = 1.24$ g/cm³, maximum dry density $\rho_{d(\max)} = 1.62$ g/cm³ and permeability $k = 8.55 \times 10^{-4}$ cm/sec. Figure 2 shows the geometry of model slope and the arrangements of linear variable differential transducers (LVDT) and pore water pressure transducers (PPT). The digital video and CCD cameras were installed above the slope surface and in front of the model test container to provide visual observation of the model slope during the centrifuge flight.

3. Experimental results

The centrifuge acceleration level was gradually increased to 28.5g where the model slope represents an approximately 11 m high slope in the prototype scale. Figures 3(a) and 3(b) show the measured pore water pressure and surface settlement, respectively. The number on the line in the Figure 3(a) represents the corresponding number of the pore

Keywords: centrifuge, ground water change, slope failure

National Institute of Occupational Safety and Health, 204-0024, Tokyo, Kiyose, Umezono 1-4-6, Tel 04-2491-4512 (Ext. 432)

water pressure transducer. During the gravity turn on process from 1g to 28.5g (t_0 to t_1) the rapid increase in surface settlement can be observed. Upon reaching the testing acceleration of 28.5g, the infiltration of rainfall was simulated by introducing water into the water supply chamber at the upslope section (at t_1). The build up of positive pore water pressure can be clearly observed in the Figure 3(a). After that the ground water level was kept constant at the elevation of 30 cm measured from the slope base (t_2 to t_3) and then the ground water level was raised again by moving up the float switch in the water supply chamber. During the increase of the ground water level, partial failure occurred at the toe of slope (t_4 to t_5). The water supply tank was then turned off and the ground water level in the water supply chamber was rapidly decreased in order to simulate the drawdown situation of ground water level during the dry period. The negative water pressures at the middle of model slope (PPT7 and PPT8) were monitored and significant increase of surface settlement was also observed. The ground water level was raised again and the failure of slope occurred from the middle portion to the top of the slope (t_6 to t_7). The rapid increase in the surface settlement can be monitored just before the failure; this phenomenon might be useful to predict the occurrence of slope failure in future. Figure 4 shows the slope model after failure, tension cracks were observed at the slope crest and shallow slip surface above the ground water level was also identified. It should be noted that this failure pattern was similar to the failure mechanism of the rainfall-induced slope failure in natural slope.

4. Conclusions

The new in-flight ground water control system was developed in this paper. The generation of positive pore water pressure and the increase of saturation of model slope due to the rise in ground water level as a result of rainwater infiltration were sufficient to trigger the slope failure. The rapid increase of the surface settlement was monitored just before the slope failure and the movement of wetting front in the slope could be observed from the variations of pore water pressure. This information is useful to establish the prediction of slope failure occurrences in the future. The effect of scaling laws of permeability should be considered in the further research to provide a better simulation and to gain more understanding about the mechanism of slope failure induced by ground water change.

Acknowledgement

The authors are grateful to Japan Society for the Promotion of Science (JSPS) for providing financial support for this research.

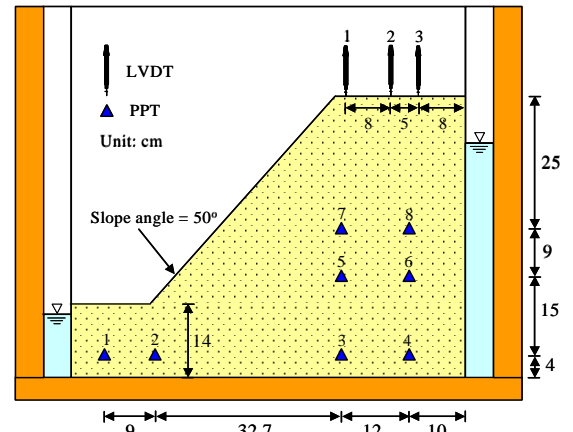


Fig. 2. Experimental set up of model slope

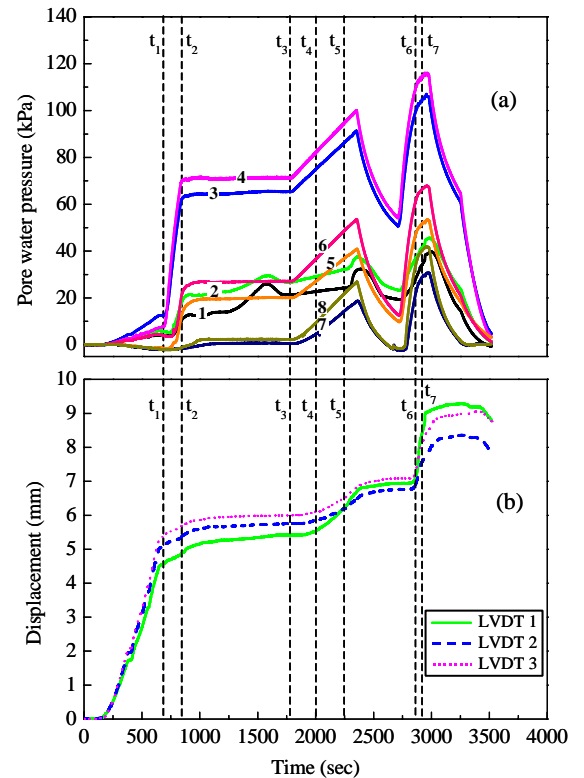


Fig. 3. Variations of (a) pore water pressure, (b) surface settlement

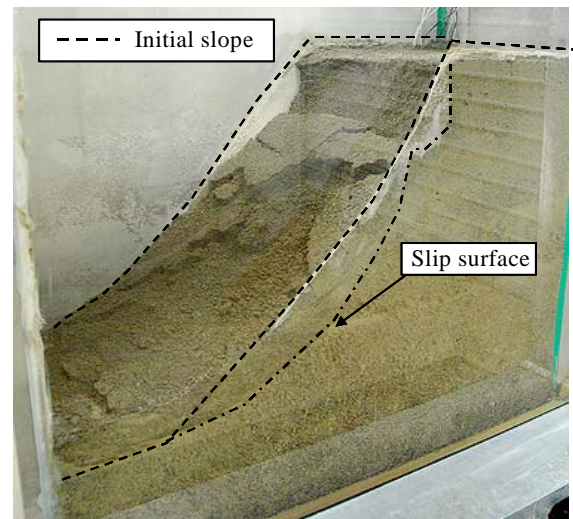


Fig. 4. Slope model after failure